

Elaiophylin Targets EIF4B to Regulate the Proliferation, Invasion, and Apoptosis of Esophageal Squamous Cell Carcinoma via the PI3K/AKT Signaling Pathway

Gao Lijuan

Renmin Hospital of Wuhan University

Chen Yongshun (✉ 2018203020082@whu.edu.cn)

Renmin Hospital of Wuhan University

Li Bin

Renmin Hospital of Wuhan University

Research Article

Keywords: Esophageal squamous cell carcinoma, PI3K/AKT, EIF4B, Migration, Proliferation, Apoptosis

Posted Date: June 15th, 2021

DOI: <https://doi.org/10.21203/rs.3.rs-604592/v1>

License:   This work is licensed under a Creative Commons Attribution 4.0 International License.

[Read Full License](#)

Abstract

Background

Esophageal cancer remains a dominating cause of cancer-associated death and has shown a sharp increase of more than 6-fold increase rates all over the world. It is divided into two main pathological types: esophageal squamous cell carcinoma (ESCC) and esophageal adenocarcinoma (EAC). Most of the patients are diagnosed at the advanced stage with distant metastasis and poor prognosis. Thus, it is urgent for us to identify new more effective drugs to improve the prognosis of patients with esophageal cancer. Elaiophylin is a novel autophagy inhibitor at the late stage, which is a C₂ symmetric macrolides separated from *Streptomyces Niger*. It was proved to have anti-tumor ability of various of cancers, yet little is known whether it could inhibit the progression of esophageal squamous cancer. The study is aimed to explore the effect of Elaiophylin on ESCC.

Methods

The protein expression level was detected by western blot assay. The viability of ESCC cells was detected by CCK8 assay. The proliferation rate was measured by ki67 immunofluorescent staining. The migratory ability of ESCC cells was identified by transwell assay. The apoptosis rate of ESCC cells was explored by Annexin V/PI analysis. And the genes might be regulated by Elaiophylin was analyzed by RNA-seq assay and verified by RT-qPCR assay. The experiments in vivo were conducted by subcutaneous into tumor in BALB/C-Nu mice.

Results

In the study, we firstly found that the Elaiophylin was a novel autophagy inhibitor in ESCC cells which is consistent with the previous studies. In addition, Elaiophylin can inhibit the proliferation and migration of ESCCs, and accelerate its apoptosis. And the activity of PI3K/AKT pathway was inhibited by Elaiophylin, the mRNA and protein expression level of EIF4B was both downregulated by Elaiophylin. Mechanistically, silencing of EIF4B could inhibit the proliferation and migration of ESCC cells and promoted apoptosis, which could be rescued by EIF4B-OE. Moreover, EIF4B overexpression suppressed the apoptosis, while increased the proliferation and migration of ESCC cells which resulted from Elaiophylin. Finally, Elaiophylin could inhibit the proliferation of esophageal cancer in vivo compared to the control group.

Conclusions

Together, our results indicated that Elaiophylin is a novel autophagy inhibitor governing growth and migratory ability of ESCC cells through PI3K/AKT signaling pathway and inhibit the proliferation of esophageal tumor in vivo. simultaneously, and identified EIF4B as a target of Elaiophylin, which might provide a new therapeutic strategy for esophageal squamous cell carcinoma.

Introduction

Esophageal cancer remains a dominating cause of cancer-associated death and has shown a sharp increase of more than 6-fold increase rates all over the world. It is divided into two main pathological types: esophageal squamous cell carcinoma (ESCC) and esophageal adenocarcinoma (EAC). Among them, the incidence of ESCC accounts for about 90%, which is the main position¹. Moreover, ESCC has a high prevalence in East Asia, eastern and southern Africa, and southern European^{2,3}. Because the early symptoms of esophageal cancer are hidden, most of the patients are diagnosed at the advanced stage with distant metastasis⁴. After surgical resection or radiotherapy and chemotherapy, due to the strong invasiveness of ESCC and the resistance of tumor tissue to drugs, the recurrence and metastasis rate is high, the prognosis is poor^{5,6}. Though the treatment has been improved, the prognosis is still very poor with overall survival rate at 5 year was 15%-25%. Thus, it is urgent to identify new more effective drugs to improve the prognosis of patients with esophageal cancer.

Elaiophylin is a novel autophagy inhibitor at the late stage, which is a C2 symmetric macrolides separated from *Streptomyces Niger*. It was firstly proved to have anti-tumor ability of ovarian cancer⁷ as well as multiple myeloma with mutant TP53⁸, yet little is known whether it could inhibit the progression of esophageal squamous cancer. EIF4B is an important component of eukaryotic transcription initiation complex, which can be recruited to the 5' untranslated region (5'UTR) of the mRNA. It was deemed to enhance the activity of eIF4A helicase to activate the function of eIF4F helicase⁹. Moreover, it can be regulated and phosphorylated by proto-oncogenic signaling pathways such as PI3K/mTOR, AKT. Moreover, eIF4B was demonstrated to regulate the translation of mRNAs which can regulate the cell proliferation and survival at the structured 5'UTR¹⁰. In recent years, eIF4B was suggested to play an important role in the progression of a various cancer cells^{11,12}.

Here, we report that Elaiophylin could inhibit the proliferation, migration of ESCC cells and provoke its apoptosis by targeting the eIF4B via PI3K/AKT signaling pathway. In the study, we firstly confirmed that the Elaiophylin was a novel autophagy inhibitor in ESCC cells which is consistent with the previous studies. In addition, Elaiophylin can inhibit the proliferation and migration of ESCCs, and accelerate its apoptosis. Then, using RNA-seq analysis to identify the genes which were regulated by Elaiophylin and verify them by RT-qPCR assay. Finally, we found the activity of PI3K/AKT pathway was inhibited by Elaiophylin. And the mRNA and protein expression level of eIF4B was both downregulated by Elaiophylin. And knockdown of EIF4B could inhibit the proliferation and migration and promote apoptosis of ESCC cells, which could be rescued by EIF4B-OE. We also found that the eIF4B overexpression could block the phenotype which was resulted from Elaiophylin. In addition, Elaiophylin could inhibit the proliferation of esophageal tumor in vivo compared to the control group. Our results suggested that the Elaiophylin might serve as a promising therapeutic medicine for esophageal squamous cell carcinoma.

Results

1. Elaiophylin is a novel autophagy inhibitor in the ESCC cells

To identify whether Elaiophylin play as an autophagy inhibitor like it does in ovarian cancer and multiple myeloma with mutant TP53, we treated ESCC cells with different concentrations. And CQ as a positive control. The western blot assay results indicated that the ratio of LC3II/LC3I was increased after exposed to Elaiophylin. And the expression level of p62 was upregulated at the protein level (Fig. 1. A). Statistical analysis of A (Fig. 1. B). We further transfected GFP-LC3 fusion protein to ESCC cells, then exposed to Elaiophylin with different concentrations. The results showed that the GFP-LC3 puncta was increased in a dose-dependent manner after Elaiophylin treated (Fig. 1. C, E). The statistical analysis of C (Fig. 1. D, F). To further verify whether Elaiophylin can inhibit the autophagy at the late stage, we transfected mCherry-GFP-LC3 plasmid to ESCC cells. Since EGFP fluorescence is quenched by acid protease in the lysosome, thus the puncta of yellow was represented of autophagosome, whereas the red was represented of autolysosome (Fig. 1. G, H). Statistical analysis of G (Fig. 1. I). The results indicated that Elaiophylin could inhibit autophagy flux at the late stage in the ESCC cells.

2. Elaiophylin exerts anti-proliferative, anti-migrative, and pro-apoptotic effects on ESCC cells

To assess the other potential function of Elaiophylin on ESCC cells, we detected the cell viability, proliferation, migration and apoptosis rate of the cells and confirmed its effect by measuring the protein expression level of E-cadherin, Bax and Bcl-2 after dealing with Elaiophylin. Utilizing the CCK8 assay, we observed that the cell viability was decreased by Elaiophylin in a dose-dependent manner in both two ESCC cell lines when compared with the control. (Fig. 2. A, B). As cancer metastasis contributed to poor prognosis of ESCC patients, transwell migration assay was also carried out to determine the effects of Elaiophylin on the ability of migration of ESCC cells. After staining with crystal violet, the inhibition of ESCC cell migration was evident, as less cell numbers were observed after treating with Elaiophylin compared to the control. (Fig. 2. C). Statistical analysis results of C (Fig. 2. D). In addition, the results of immunofluorescent staining for Ki67 showed that the Ki67 positive cells was decreased by Elaiophylin, which indicated that the proliferation rate of ESCC cells was attenuated (Fig. 2. E, G). Statistical analysis results of E, G (Fig. 2. F, H). Notably, flow cytometry assay established increased apoptosis rates in ESCC cells by treating with Elaiophylin (Fig. 2. I). Statistical analysis results of I (Fig. 2. J). Moreover, western blot assay analysis showed increased protein expression of E-cadherin, Bax by Elaiophylin, whereas the Bcl-2 expression level was decreased (Fig. 2. K, L, M).

3. RNA-seq results indicated that Elaiophylin could inhibit the activation of PI3K/AKT signaling pathway

To elucidate the mechanism and target of Elaiophylin, we conducted RNA-seq analysis (GSE171167) to identify the genes that were transcriptionally affected by Elaiophylin. In RNA-seq, the correlation of expression levels between samples is an important indicator to test the reliability of the experiment and whether the sample selection is reasonable. The closer the correlation coefficient is to 1, the higher the similarity of the expression patterns between samples. The Encode plan recommends that the square of Pearson's correlation coefficients of the two biological replicates in each group of the two cell lines are both greater than 0.97, indicating that the sample has good reproducibility and the sequencing results are credible (Fig. 3. A, F). Then the differently expressed genes were screened, and the screening criterion was $|\log_2(\text{FoldChange})| \geq 1$ and $\text{padj} \leq 0.05$. The volcano chart shows the distribution of differential genes for each comparison combination (Fig. 3. B, G). Red dots indicate genes that are up-regulated, and green dots indicate genes that are down-regulated. The results showed that there were 360 up-regulated genes and 891 down-regulated genes in Eca109 cells (Fig. 3. B). And there are 126 up-regulated genes and 435 down-regulated genes in KYSE450 cells (Fig. 3. G). Then cluster all differentially expressed genes. The differential genes of all comparison groups are combined as the differential gene set. We use mainstream hierarchical clustering to perform cluster analysis on the FPKM value of genes, and perform uniform processing on the rows. Shown in the form of a heat map. Genes with similar expression patterns in the heat map will be grouped together. The color in each grid is the value obtained after the row of expression data is normalized. Therefore, the colors in the heat map can only be compared horizontally, not vertically. The results showed that in the two cell lines, the expression levels of differentially expressed genes in different samples were significantly different (Fig. 3. C, H). Finally, we used clusterProfiler software to perform GO (Gene Ontology) function enrichment analysis for differential genes, and KEGG (Kyoto Encyclopedia of Genes and Genomics) function enrichment analysis. GO is a comprehensive database describing gene function, divided into three parts: biological process and cell composition, and molecular function. We mainly focus on the enrichment analysis of biological processes. Figure 3D mainly shows the results of the enrichment analysis of the biological process of Eca109 cells. The abscissa in the figure represents the ratio of the number of differential genes annotated to GO Term to the total number of differential genes, the ordinate is GO Term, and the size of dot represents the annotation to GO the number of genes on Term, the color from red to purple represents the significance of enrichment. The results showed that in the two kinds of cells, Elaiophylin mainly affected the binding of intercellular cadherin molecules and intercellular adhesion molecules (Fig. 3. D, I). KEGG enrichment results show that the abscissa is the ratio of the number of differential genes, the ordinate is the KEGG pathway, the size of the dot represents the number of genes annotated to the KEGG pathway, and the color from red to purple represents enrichment. The results show that Elaiophylin mainly affects the PI3K-Akt signaling pathway in the two cell lines (Fig. 3. E, J).

4. Elaiophylin might suppress the expression of EIF4B via PI3K/AKT signaling pathway

In order to analyze the genes that were downregulated by Elaiophylin both in Eca109 and KYSE450 cells, we firstly found the common DEGs by Venn (Fig. 4. A). Then we annotated the downregulation DEGs to GO (Fig. 4. B) and KEGG (Fig. 4. C) analysis, as predicted, the results showed that the genes were mostly enrichment in the PI3K-Akt signaling pathway. Hence, we verified the genes enrichment in PI3K-Akt pathway by RT-qPCR assay. Noteworthy is that the expression of COL4A1, EIF4B, ITGA5 and ITGB1 was blocked at the mRNA level both in the Eca109 and KYSE450 cells (Fig. 4. D, E). Since EIF4B was previously reported to play an essential role in cell proliferation and survival, especially in cancer cells, but has not been explored in esophageal cancer, we therefore checked the EIF4B protein expression. Furthermore, we also assessed the PI3K, p-PI3K, AKT, p-AKT protein expression level. Finally, we observed that the EIF4B, p-PI3K, AKT, p-AKT protein expression level was downregulated by Elaiophylin, which further confirmed that the activity of PI3K-AKT signaling pathway was inhibited (Fig. 4. F). Taken together, from what discussed before, we speculated that Elaiophylin might target to EIF4B to regulate the proliferation, migration and apoptosis of ESCC cells.

5. Knockdown of EIF4B suppresses the proliferation, migration of ESCC cells and promotes apoptosis

To further confirm the function of EIF4B in ESCC cells, we continue knocked down the EIF4B in ESCC cells to test if silencing EIF4B affect its proliferation, migration and apoptosis. All cells were divided into three groups, scramble, shEIF4B and shEIF4B + EIF4B-OE. First of all, western blot assay was employed to detect the EIF4B expression across all groups, the results demonstrated that the EIF4B was effectively knocked down after transfection of shEIF4B, and was reversed by co-transfection with EIF4B-OE (Fig. 5. A, B). Transwell assay showed that the migratory ability was attenuated when silencing the EIF4B, and can be reversed by co-transfection with EIF4B-OE (Fig. 5. C, D). And efficient shRNA-directed knockdown of EIF4B expression could inhibit the proliferation of Eca109 and KYSE450 cells, as the percentage of ki67 positive cells was decreased in the shEIF4B group compared to scramble and shEIF4B + EIF4B-OE group (Fig. 5. E, F, G, H). Using Annexin V-FITC/PI assay, we also observed that effective knockdown of EIF4B could accelerate the apoptosis of ESCC cells compared to the scramble and shEIF4B + EIF4B-OE group (Fig. 5. I, J). Additionally, western blot assay examined the protein expression of E-cadherin, Bax, and Bcl-2, the results showed that E-cadherin, Bax was upregulated when silencing EIF4B and Bcl-2 was downregulated, which was reversed by overexpression of EIF4B (Fig. 5. K, L). All the data suggested that knockdown of EIF4B could inhibit the proliferation and migration of ESCC cells and promotes its apoptosis. Whereas, overexpression of EIF4B on the basis of blocking the expression of EIF4B abrogated the effect of silencing of EIF4B, which indicated that the EIF4B might play an important role in ESCC progression.

6. Upregulation of EIF4B could rescued the phenotype on ESCC cells caused by Elaiophylin

To ascertain whether the Elaiophylin affects the ability of proliferation, migration and apoptosis of ESCC cells via EIF4B, we transfected eIF4B-OE plasmid to ESCC cells on the basis of treating with Elaiophylin. All cells were divided to three groups vector, Elaiophylin only and EIF4B-OE on the basis of Elaiophylin. Firstly, the EIF4B protein expression level was examined by western blot, the result indicated that it was down regulated by Elaiophylin, but was reversed by co-transfection of EIF4B-OE. (Fig. 6. A, B). The transwell migration assay showed that transfection with EIF4B-OE could blocked the migration-inhibitory effect resulted from Elaiophylin (Fig. 6. C, D). Interestingly, the IHC of ki67 of the different groups illustrated that the transfection with EIF4B-OE on the basis of Elaiophylin could enhance the proliferation of Eca109 and KYSE450 cells when compared with the Elaiophylin only group. (Fig. 6. E, F, G, H). In addition, the cell apoptosis rate was also decreased when transfection with EIF4B-OE on the basis of Elaiophylin compared to the Elaiophylin only group as detected by flow cytometry (Fig. 6. I, J). In the end, in order to confirm the effect of different groups on the proliferation, migration and apoptosis in Eca109 and KYSE450 cells, the protein level of E-cadherin, Bax, Bcl-2 was examined by western blot analysis. The result showed that the expression level of E-cadherin, Bax, Bcl-2 in the Elaiophylin group was reversed by transfection of EIF4B-OE (Fig. 6. K, L). The phenomenon indicated that eIF4B-OE could reverse the effect of the Elaiophylin on ESCC cells.

7. Elaiophylin inhibit the growth of esophageal tumor in vivo

As Elaiophylin could inhibit the proliferation of ESCC cells in the vitro, we further investigated the effect of Elaiophylin on tumor growth in vivo. The Eca109 cell line was used to inject into the right flanks of nude mice to construct an in vivo model. After two weeks, Elaiophylin was given i.p. (1mg/kg) every two days for 21 days, or DMSO was used as a control. Finally, the tumors were taken from the mice, weighted and photographed followed by measurement of the volume (Fig. 7. A, B, C). We found that the Elaiophylin group was lighter and smaller than the control group. In a word, these results suggest that Elaiophylin could inhibit the progression of esophageal tumor in vivo.

Discussion

Previous studies have reported that Elaiophylin was a novel autophagy inhibitor and showed potent antitumor activity in many kinds of tumors. For instance, Elaiophylin exerted prominent antitumor efficacy as an autophagy inhibitor in ovarian cancer⁷ and multiple myeloma with mutant TP53, which was also involved ER stress-associated apoptosis⁸. Besides, Elaiophylin could inhibit tumor progression and suppressed tumor growth in xenograft of metastatic castration-resistant prostate cancer (mCRPC), which was targeting the orphan nuclear receptor ROR γ ¹³. On the other hand, Elaiophylin has also been proved to inhibit angiogenesis in cancers as well as proliferation, migration and invasion accompanied by it. However, little is known about the function of Elaiophylin in ESCC. Our findings that Elaiophylin inhibits the autophagy at the late stage is in line with the previous reports reported in ovarian cancer⁷ as well as

multiple myeloma with mutant TP53⁸. In addition, our results showed that Elaiophylin could inhibit the proliferation and migration of ESCC cells and promotes its apoptosis.

The eukaryotic initiation factor 4B (EIF4B) phosphorylation can be stimulated by PI3K/AKT/mTOR signaling pathways¹¹, which is on Ser422¹⁴. In relation to this, we identified that the EIF4B was inhibited by the suppression of PI3K/AKT signaling pathway in ESCC cells. An increasing number of studies have also indicated that EIF4B is necessary for cell proliferation and survival, and its effect is achieved by regulating the translation of proliferation and survival-related mRNA¹⁵. And EIF4B can play an important anti-apoptotic effect in acute leukemia cells by regulating the expression of anti-apoptotic proteins Bcl-2 and Bcl-xl. According to the relevant studies, knockdown of EIF4B can reduce the rate of cell proliferation, promote caspase-dependent apoptosis, and make cells more sensitive to camptothecin-induced cell death. EIF4B can inhibit the apoptosis of acute leukemia cells¹¹. And EIF4B can promote the proliferation and metastasis of hepatocellular carcinoma¹². MiR-216a can inhibit the development of oral squamous cell carcinoma¹⁶ and non-small cell lung cancer¹⁷ by targeting EIF4B. Intriguingly, it was recently reported that EIF4B was also shown to be a novel marker for poor prognosis of diffuse large B-cell lymphoma¹⁸. All of the results indicated that EIF4B is closely associated with the occurrence and progression of a various of tumors. According to the RNA-seq analysis, when dealing the ESCC cells with Elaiophylin the activity of PI3K/AKT signaling pathway was negatively regulated. At the same time, the expression of EIF4B was also downregulated at both the mRNA and protein level.

In addition, given that EIF4B can regulate the proliferation and survival of many kinds of cancers. We further knockdown the EIF4B of ESCC cells, which contributed to the lower proliferation and migration and higher apoptosis rate. Meanwhile, in combination with a EIF4B-OE vector on the basis of silencing of EIF4B, the effect of downregulation of EIF4B on ESCC cells is offset, which indicated that silencing EIF4B could inhibit the proliferation and migration of ESCC cells and promote apoptosis. Of note, forced EIF4B expression blocked the effect of Elaiophylin and had an effective promotion ability of proliferation and migration and inhibition of apoptosis of ESCC cells. The results of our study showed that EIF4B might be a target of Elaiophylin to regulate the proliferation, migration and apoptosis of ESCC cells. To further verify our results, we conducted the experiments *in vivo*. The results showed that Elaiophylin could meanwhile inhibit the growth of esophageal tumor *in vivo*.

In summary, in this study we firstly found that Elaiophylin could serve as a novel autophagy inhibitor in ESCC cells. In addition, our results indicated that knockdown of EIF4B could inhibit the proliferation, migration of ESCC cells and promote apoptosis, which was could blocked by EIF4B-OE. Then we revealed that EIF4B has an opposite effect of Elaiophylin and EIF4B-OE further rescued the effect of Elaiophylin on ESCC cells, which indicated that Elaiophylin could meanwhile target EIF4B via PI3K/AKT signaling pathway to inhibit the viability, proliferation and migration of ESCC cells and to promote its apoptosis. Moreover, Elaiophylin could inhibit the growth of esophageal tumor *in vivo*. In conclusion, our study identified that Elaiophylin may serve as a new therapeutic medicine for ESCC patients, and improve patient outcomes.

Materials And Methods

Cell culture, antibodies and reagents

Eca109 and KYSE450 cell lines were obtained from ATCC (American Type Culture Collection), and cultured in RPMI-1640 medium supplemented with 10% fetal bovine serum, 100U/ml penicillin and 100µg/ml streptomycin at 37°C in a humidified air of 5% CO₂ saturation. Both cell lines were authenticated by STR and tested for mycoplasma contamination. EIF4B Rabbit Polyclonal antibody (17917-1-AP), AKT Rabbit Polyclonal antibody (10176-2-AP), Phospho-AKT (Ser473) Mouse Monoclonal antibody (66444-1-Ig), PI3 Kinase p85 Alpha Mouse Monoclonal antibody (60225-1-Ig), LC3 Rabbit Polyclonal antibody (14600-1-AP), P62/SQSTM1 Rabbit Polyclonal antibody (18420-1-AP), E-cadherin Rabbit Polyclonal antibody (20874-1-AP), BAX Rabbit Polyclonal antibody (50599-2-Ig), BCL2 Rabbit Polyclonal antibody (12789-1-AP) were purchased from Proteintech. The Phospho-PI3KP85α/γ/β-Y467/Y199/Y464 Rabbit Phosphorylated Antibodies (AP0854), ACTB Rabbit mAb (AC026), GAPDH Mouse mAb (AC002) were purchased from ABclonal. The Cell Counting Kit-8 and Crystal Violet Staining Solution were purchased from Beyotime. The FITC Annexin V Apoptosis Detection Kit I (556547) was purchased from BD Pharmingen. The Corning Costar Transwell, pore size 8.0µm was purchased from Corning.

Protein extraction and Western blot assay

The cells which pretreatment with Elaiophylin or transfection with vectors were collected by 200µL loading buffer followed by warming at 100°C for 10min. The protein concentration in the supernatants was detected by standard bicinchoninic acid (BCA) method. The proteins were loaded onto a 10% sodium dodecyl sulfate polyacrylamide gel, and proteins were separated by electrophoresis. Then, the proteins were transferred onto a polyvinylidene fluoride (PVDF) membrane with a constant current of 200mA at 2h and blocked with 10% non-fat milk at room temperature for 1h. Afterwards, recycling the milk and washing the membrane with Tris-buffered saline with 0.1% v:v Tween 20, the membranes were incubated with the anti-PI3K, anti-p-PI3K, anti-AKT, anti-p-AKT, anti-EIF4B, anti-E-cadherin, anti-Bax, anti-Bcl-2 antibodies overnight at 4°C. After washing the membranes with TBST 10min three times, the membranes were subsequently incubated with the second antibody horseradish peroxidase-conjugated immunoglobulin G for 1h at room temperature. The results of the expression level of proteins were detected by enhanced chemiluminescence (ECL) kit and developed by x-ray film in the darkroom. And the semi-quantitative analysis of relative expression of proteins normalized to GAPDH or ACTIN was conducted by Image J Fiji software system.

Immunofluorescence cell staining of Ki67

After cell counting, we added 50,000 cells to each climbing piece. After 24h, wash the cells with PBS three times and fixed them with 4% paraformaldehyde and permeabilized them with 0.5% Triton X-100 for

20min at the room temperature. Then blocked the cells with 5% goat serum for 30min, and followed by incubating with primary antibodies overnight at 4°C. Next day, recycled the primary antibodies and washed the cells with PBS three times. Then incubated the cells with fluorescein isothiocyanate-labeled secondary antibodies for 1h at the room temperature. Whereafter, washed the cells with PBS three times once again and incubated with DAPI for 2min. Following by washing with PBS one time, used absorbent paper to absorb the liquid on the slide and mounted the slide with a mounting solution containing anti-fluorescence quencher and then observed and collected the image under a laser scanning confocal microscope.

Cell counting kit (CCK)-8 assay

The Eca109 and KYSE450 cells were seeded in 96 well plates at a density of 8,000 and 10,000 cell per well respectively. All cells were divided into blank groups, untreated control groups and different concentrations of Elaiophylin for 12h groups. All samples were incubated in an 5% CO₂, humidified atmosphere at 37°C. Every group was established three holes. Subsequently, 10μL CCK-8 solution was added to each well with 100μL medium and incubated for 30min in an 5% CO₂, humidified atmosphere at 37°C. Finally, the absorbance was detected at the wavelength by using microplate reader.

Transwell migration assay

When the esophageal squamous carcinoma cells were grown to 80%-90% confluence, the cultured medium was removed, following washed with pre-cold PBS, we starved the cells with EBSS for 3h. Then, the cells were digested by 0.25% trypsin, and resuspended in starvation medium with non-FBS. After cell counting, 1×10⁵ cells were added on the top of the chambers and filled the bottom room of the chambers with medium containing 10% FBS. After cultivated for 24h, cells migrated to the other side of the insert. Subsequently, the 500μL PFA was added to the insert of chamber to fix the cells, followed by staining with crystal violet for 10min and dried at the room temperature. Finally, counted the number of cells passing through the chamber in each experimental group under the microscope.

Quantitative Real-time PCR assay

Following treatment with Elaiophylin, the total RNA was extracted by Trizol reagent according to the manufacturer's instruction. And the total RNA was reverse-transcribed by using HiScript® II Reverse Transcriptase kit. qPCR amplification was conducted using the SYBR Green PCR Master Mix. The thermal profile of reverse transcription was 50°C for 15min followed by 85°C 5 sec. Then cDNA product obtained before was used to qPCR following the thermocycling parameters of 95°C for 2min, 40 amplification cycles of 95°C for 5s, and 60°C for 30s. The relative quantification of the expression levels of the target genes were normalized to β-ACTIN. The primers of Actin are forwards 5'-CTCTTCCAGCCTTCCTCCT-3', and reverse, 5'-AGCACTGTGTTGGCGTACAG-3'. The primers of EIF4B are forwards 5'-

AGGGGAAGACTATCTCCCTAACA-3', and reverse, 5'-TCATCCGTTTCATCAGCCCAG-3'. The primers of ITGB1 are forwards 5'-GTAACCAACCGTAGCAAAGGA-3', and reverse, 5'-TCCCCTGATCTTAATCGCAAAC-3'. The primers of ITGA6 are forwards 5'-ATGCACGCGGATCGAGTTT-3', and reverse, 5'-TTCCTGCTTCGTATTAACATGCT-3'. The primers of COL4A1 are forwards 5'-ACTCTTTTGTGATGCACACCA-3', and reverse, 5'-AAGCTGTAAGCGTTTTCGTA-3'. The expression level of targeted genes were normalized by ΔCt and the relative fold changes were calculated by the $2^{-\Delta\Delta\text{Ct}}$.

Cell apoptosis detected by flow cytometry assay

The apoptosis rate of Eca109 and KYSE450 cells was detected by fluorescein isothiocyanate (FITC) Annexin V/propidium iodide (PI) kit according to the manufacturer's instructions. The esophageal squamous carcinoma cells were seeded into 6cm dish at a density of 5×10^5 cells, and treatment with different concentration of Elaiophylin and transfected with plasmids. Wash the adherent cells with cold PBS, and digested with 0.25% trypsin without EDTA for 5min, then resuspended the cell with in medium. After centrifugation, washing the cells twice with cold PBS. Subsequently, resuspended the cells with 100 μL binding buffer and added 5 μL of Annexin V-FITC and propidium iodide into each tubes. After incubating it 15min at room temperature out of light, the samples were detected by flow cytometry within 1h by using Cytoflex.

Xenograft mice model

The male BALB/C-Nu mice (5–7 weeks old) was brought from HUNAN SJA LABORATORY ANIMAL CO., LTD. (Hunan China), all animal experiments were performed in strict accordance with the guidelines of the Research Ethics Committee of Wuhan university. All experimental protocols were approved by Ethics Committee of Wuhan University. Number: MLICJ2021013. Approval Number: MRI2021-LACJ013. Eca109 cells (5×10^6) resuspended in 200 μL of PBS were injected subcutaneously into the right flanks of nude mice. After two weeks, Elaiophylin was given i.p. (1mg/kg) every two days for 21 days, or DMSO was used as a control. Finally, the xenograft tumors were removed and weighted. Tumor volumes were calculated as $\text{length} \times (\text{square of width}) / 2$. The study is reported in accordance with ARRIVE guidelines.

Statistical analysis

All experiments were performed at least three times. All data was presented as means \pm SEM. P value < 0.05 was considered significantly different. Statistical comparisons between two groups were made using Student's t-test. Statistical analysis and graphs were produced using GraphPad Prism 8 software.

Declarations

Acknowledgment

None

Conflicts of interest

None

Authors' contributions

Chen Yongshun have made substantial contributions to the conception, Gao Lijuan contributes to the design of the work and drafted the work and substantively revised it. LiBin contributes to the creation of new software used in the work. All authors read and approved the final manuscript.

References

1. Domper Arnal, M. J., Ferrández Arenas, Á. & Lanas Arbeloa, Á. Esophageal cancer: Risk factors, screening and endoscopic treatment in Western and Eastern countries. *World J Gastroenterol* **21**, 7933-7943, doi:10.3748/wjg.v21.i26.7933 (2015).
2. Short, M. W., Burgers, K. G. & Fry, V. T. Esophageal Cancer. *Am Fam Physician* **95**, 22-28 (2017).
3. Lin, Y.*et al.* Esophageal cancer in high-risk areas of China: research progress and challenges. *Ann Epidemiol* **27**, 215-221, doi:10.1016/j.annepidem.2016.11.004 (2017).
4. Wang, M., Smith, J. S. & Wei, W. Q. Tissue protein biomarker candidates to predict progression of esophageal squamous cell carcinoma and precancerous lesions. *Ann N Y Acad Sci* **1434**, 59-69, doi:10.1111/nyas.13863 (2018).
5. Hirano, H. & Kato, K. Systemic treatment of advanced esophageal squamous cell carcinoma: chemotherapy, molecular-targeting therapy and immunotherapy. *Jpn J Clin Oncol* **49**, 412-420, doi:10.1093/jjco/hyz034 (2019).
6. Lam, A. K. Introduction: Esophageal Squamous Cell Carcinoma-Current Status and Future Advances. *Methods Mol Biol* **2129**, 1-6, doi:10.1007/978-1-0716-0377-2_1 (2020).
7. Zhao, X.*et al.* Elaiophylin, a novel autophagy inhibitor, exerts antitumor activity as a single agent in ovarian cancer cells. *Autophagy* **11**, 1849-1863, doi:10.1080/15548627.2015.1017185 (2015).
8. Wang, G.*et al.* The novel autophagy inhibitor elaiophylin exerts antitumor activity against multiple myeloma with mutant TP53 in part through endoplasmic reticulum stress-induced apoptosis. *Cancer Biol Ther* **18**, 584-595, doi:10.1080/15384047.2017.1345386 (2017).
9. Andreou, A. Z. & Klostermeier, D. eIF4B and eIF4G jointly stimulate eIF4A ATPase and unwinding activities by modulation of the eIF4A conformational cycle. *J Mol Biol* **426**, 51-61, doi:10.1016/j.jmb.2013.09.027 (2014).
10. Andreou, A. Z., Harms, U. & Klostermeier, D. Single-stranded regions modulate conformational dynamics and ATPase activity of eIF4A to optimize 5'-UTR unwinding. *Nucleic Acids Res* **47**, 5260-

5275, doi:10.1093/nar/gkz254 (2019).

11. Ma, Y.*et al.* [Synergistic role of JAK/STAT5 and PI3K/AKT signaling pathways in regulating eIF4B in acute leukemia]. *Sheng Wu Gong Cheng Xue Bao* **36**, 2413-2423, doi:10.13345/j.cjb.200015 (2020).
12. Xu, J.*et al.* Long noncoding RNA GMAN promotes hepatocellular carcinoma progression by interacting with eIF4B. *Cancer Lett* **473**, 1-12, doi:10.1016/j.canlet.2019.12.032 (2020).
13. Zheng, J.*et al.* Targeting castration-resistant prostate cancer with a novel ROR γ antagonist elaiophylin. *Acta Pharm Sin B* **10**, 2313-2322, doi:10.1016/j.apsb.2020.07.001 (2020).
14. Bettegazzi, B.*et al.* eIF4B phosphorylation at Ser504 links synaptic activity with protein translation in physiology and pathology. *Sci Rep* **7**, 10563, doi:10.1038/s41598-017-11096-1 (2017).
15. Shahbazian, D., Parsyan, A., Petroulakis, E., Hershey, J. & Sonenberg, N. eIF4B controls survival and proliferation and is regulated by proto-oncogenic signaling pathways. *Cell Cycle* **9**, 4106-4109, doi:10.4161/cc.9.20.13630 (2010).
16. Li, L. & Ma, H. Q. MicroRNA-216a inhibits the growth and metastasis of oral squamous cell carcinoma by targeting eukaryotic translation initiation factor 4B. *Mol Med Rep* **12**, 3156-3162, doi:10.3892/mmr.2015.3761 (2015).
17. Wang, R. T., Xu, M., Xu, C. X., Song, Z. G. & Jin, H. Decreased expression of miR216a contributes to non-small-cell lung cancer progression. *Clin Cancer Res* **20**, 4705-4716, doi:10.1158/1078-0432.Ccr-14-0517 (2014).
18. Horvilleur, E.*et al.* A role for eukaryotic initiation factor 4B overexpression in the pathogenesis of diffuse large B-cell lymphoma. *Leukemia* **28**, 1092-1102, doi:10.1038/leu.2013.295 (2014).

Figures

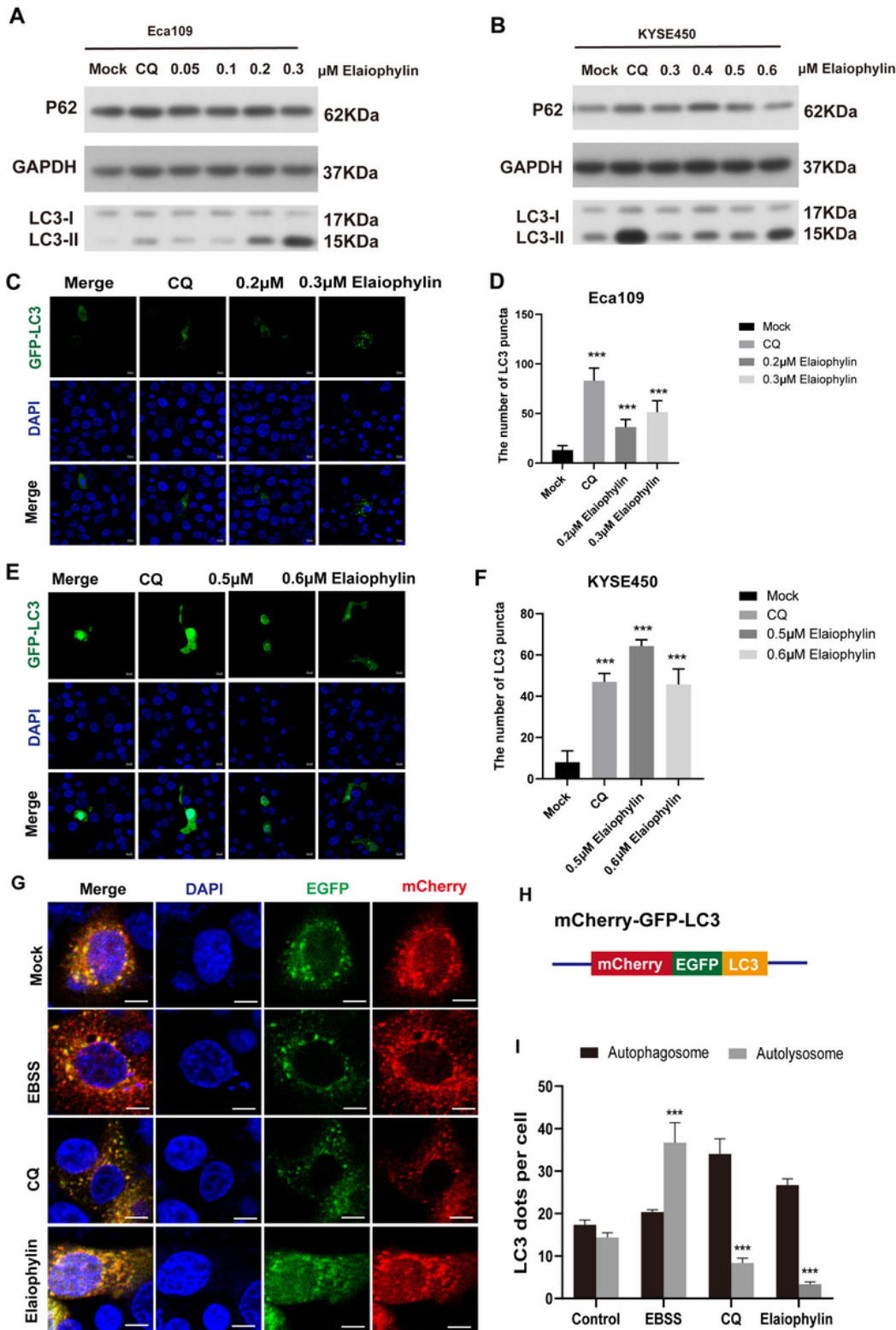


Figure 1

Elaiophylin could inhibit autophagy flux at the late stage in the ESCC cells. (A, B) Western Blot assay was carried out to detect the level of LC3 and p62 protein in Eca109 and KYSE450 following treatment with different concentrations of Elaiophylin. The grouping of gels cropped from different parts of the same gel and the same exposures. (C, E) The LC3 puncta in Eca109 and KYSE450 cells was visualized by confocal microscope after transfected with GFP-LC3 fusion protein. (D, F) Statistical analysis of C, E. Error bars

represent the mean±SEM. (G) After transfected with mCherry-EGFP-LC3 plasmids followed by treatment with Elaiophylin, the puncta of LC3 were visualized by confocal microscope, the scale bar was 10µm. The puncta of yellow are represented of autophagosome, whereas the red was represented of autolysosome. (H) The structure of the mCherry-EGFP-LC3 plasmids. (I) Statistical analysis of autolysosome compared with the autophagosome. Error bars represent the mean±SEM. Statistical analysis was generated from unpaired t-test, asterisks denote statistical significance as ***p<0.001.

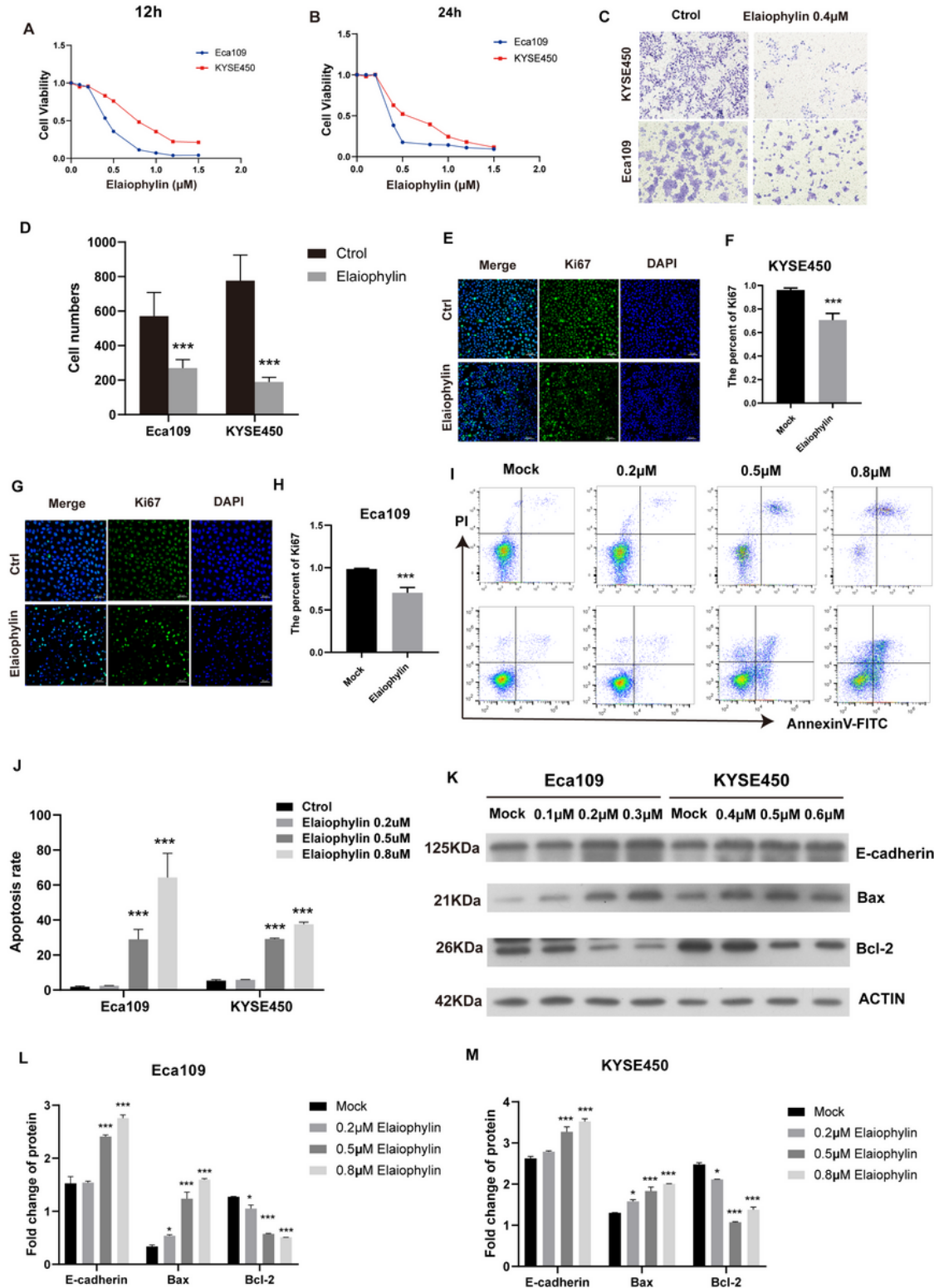


Figure 2

Elaiophylin exerts anti-proliferative, anti-migrative, and pro-apoptotic effects on ESCC cells. (A, B) The CCK-8 assay was utilized to explore the effect of Elaiophylin on the proliferation of Eca109 and KYSE450 cells. (C) The migration ability between the control and Elaiophylin group was detected by transwell assay. (D) Statistical analysis of the cell numbers migrated to the other side of the chamber. Error bars represent the mean±SEM. (E, G) IHC of ki67 was used to detect the proliferation rate of Eca109 and KYSE450 cells following by treatment with Elaiophylin. (F, H) Statistical analysis result of the IHC showed that the ki67 expression level was downregulated in the Elaiophylin group compared with the control. Error bars represent the mean±SEM. (I) The apoptosis rate was measured by Annexin V/PI in Eca109 and KYSE450 cells. Cells with Annexin V-FITC positive and PI negative or both Annexin V-FITC and PI positive were considered apoptotic. (J) Statistical analysis of the apoptosis rate of the two cells. Error bars represent the mean±SEM. (K) The protein level of E-cadherin, Bax, Bcl-2 was measured in Eca109 and KYSE450 cells after treatment with different concentrations of Elaiophylin. The E-Cadherin, Bax, Actin was cropped from different parts of the same gel, and Bcl-2 was from different gels and from the same exposures. (L, M) Statistical analysis of the protein expression in K. Error bars represent the mean±SEM. Statistical analysis was generated from unpaired t-test, asterisks denote statistical significance as *p<0.05, ***p<0.001.

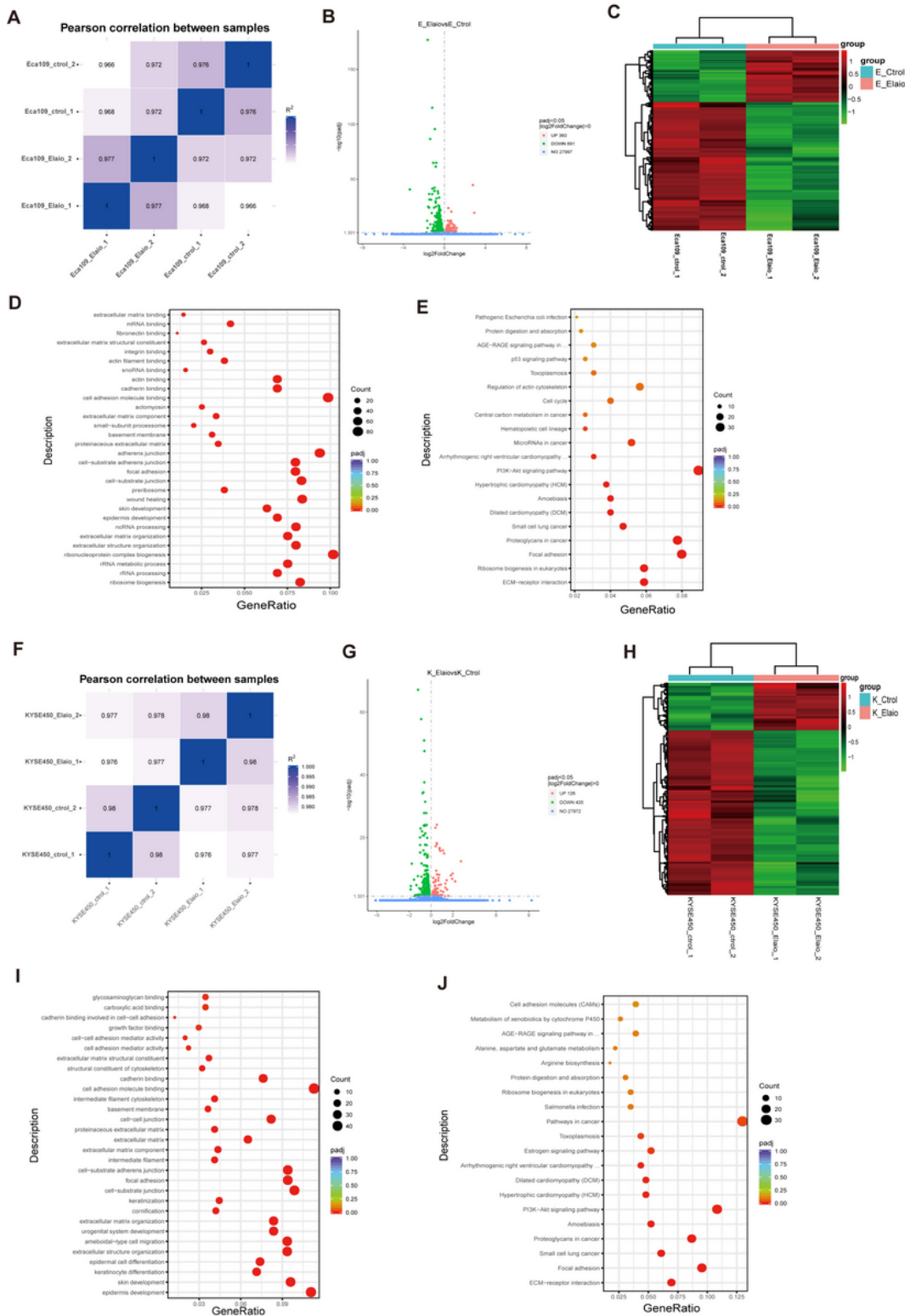


Figure 3

RNA-seq analysis of the Eca109 and KYSE450 cells after treatment of Elaiophylin for 12h. (A, F) Heat map showing the hierarchically clustered Pearson correlation matrix resulted from comparing the transcript expression values of the control and Elaiophylin samples in Eca109 and KYSE450 cells respectively. (B, G) Identification of Elaiophylin regulated genes in Eca109 and KYSE450 cells. Upregulated genes are labelled in red, whereas downregulated genes are labelled in blue in the volcano

plot. (C, H) Hierarchical clustering of DEGs in control and Elaiophylin samples in Eca109 and KYSE450 cells. FPKM values are log2-transformed and then median-centred by each gene. (D, I) The top 30 representative GO biological processes of Elaiophylin downregulated genes in Eca109 and KYSE450 cells. (E, J) The top 30 representative KEGG pathways of Elaiophylin regulated genes in Eca109 and KYSE450 cells.

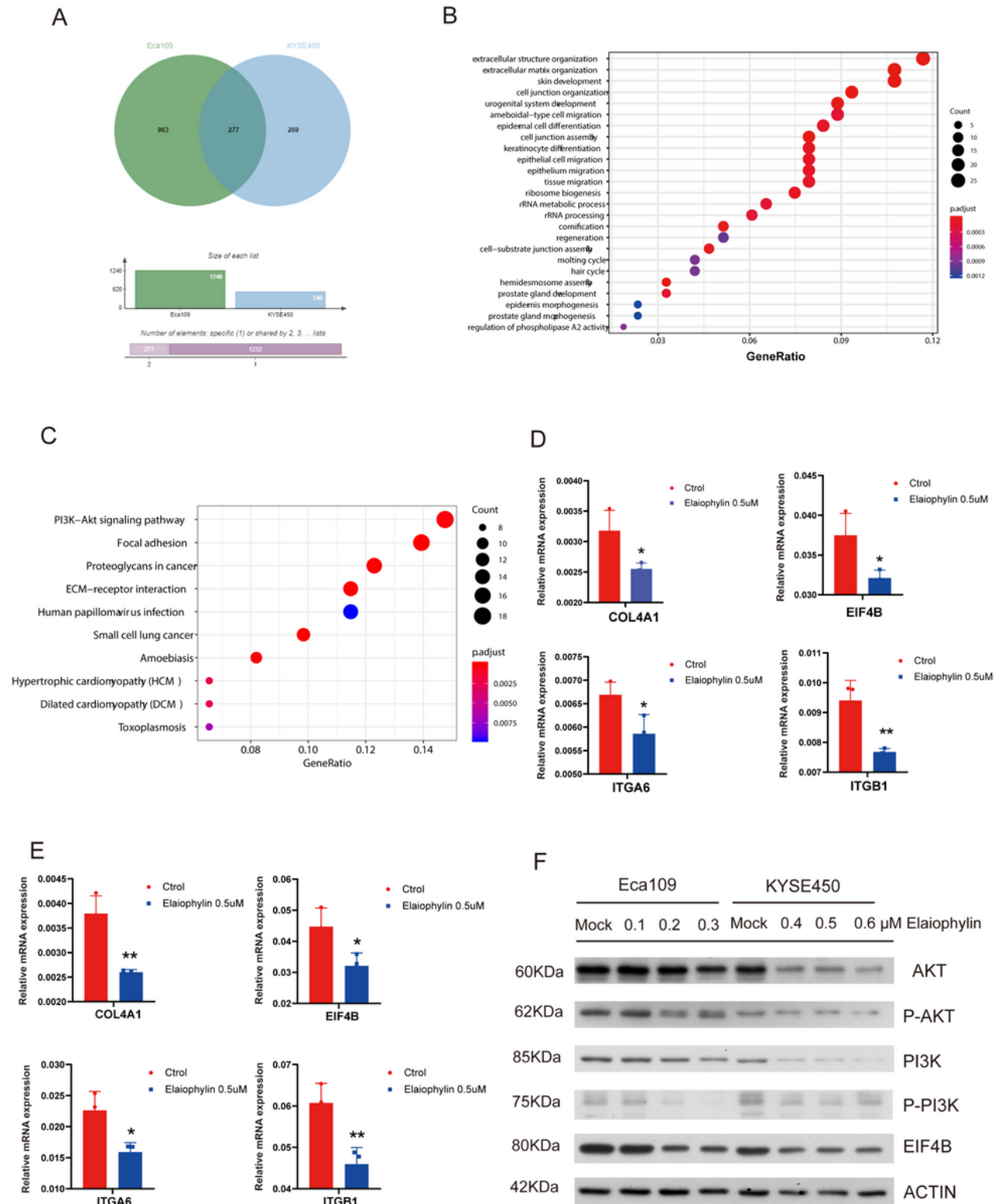


Figure 4

Verification of the genes and proteins that might regulated by Elaiophylin. (A) Venn diagram showed the overlaps the downregulated genes both in Eca109 and KYSE450 cells exposed to Elaiophylin. (B) GO analysis of the down DEGs. (C) KEGG analysis of the down DEGs. (D, E) The mRNA levels of COL4A1, EIF4B, ITGA6, ITGB1 in Eca109 was quantified by qRT-PCR normalized to Actin. The expression level levels were calculated using $2^{-\Delta\Delta CT}$ method. Error bars represent the mean \pm SEM. (F) The protein level of AKT, p-AKT, PI3K, P-PI3K, EIF4B in Eca109 and KYSE450 cells treated by different concentration of Elaiophylin were analyzed by Western blot assay. The grouping of gels cropped from different gels and same exposures. In both cell lines, the AKT, p-AKT, PI3K, P-PI3K, EIF4B protein were consistently downregulated by Elaiophylin. ACTIN was used as loading control. Error bars represent the mean \pm SEM. Statistical analysis was generated from unpaired t-test, asterisks denote statistical significance as *p \leq 0.05, **p \leq 0.01.

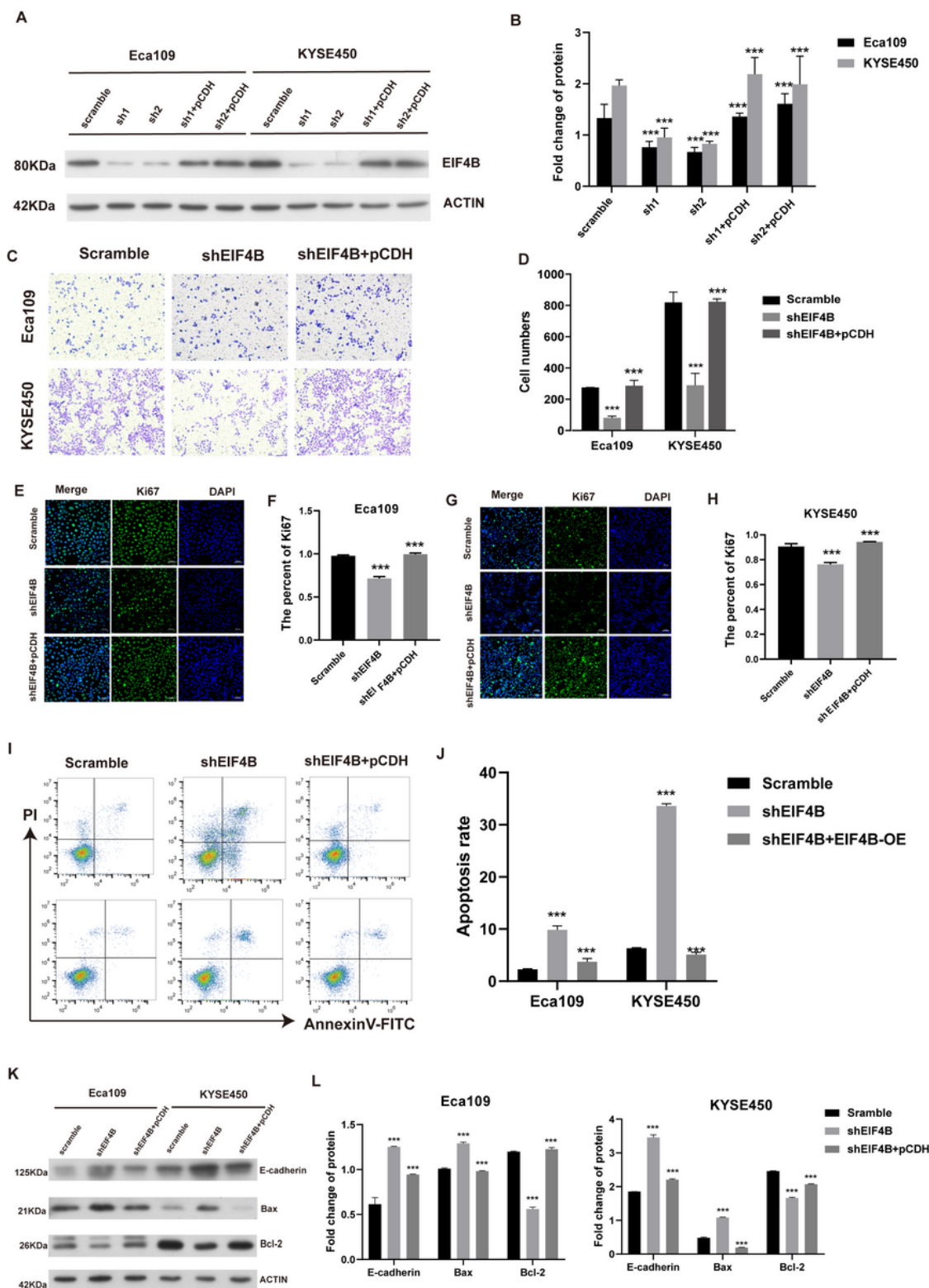


Figure 5

Knockdown of EIF4B suppresses the proliferation, migration of ESCC cells and promotes apoptosis. (A) Western blot examined the protein expression of EIF4B across different groups. (B) Statistical analysis of the protein expression of EIF4B. Error bars represent the mean±SEM. (C) Transwell assay measured the migration ability across different groups. (D) Statistical analysis of the cell numbers migrated to the other side of the chamber. Error bars represent the mean±SEM. (E, G) IHC of ki67 was used to detect the

proliferation rate of Eca109 and KYSE450 cells across different groups. (F, H). Statistical analysis result of the IHC showed that the ki67 expression level was downregulated in the Elaiophylin group compared with the control, and could be reversed by EIF4B-OE. Error bars represent the mean±SEM. (I) The apoptosis rate was measured by Annexin V/PI in Eca109 and KYSE450 cells. Cells with Annexin V-FITC positive and PI negative or both Annexin V-FITC and PI positive were considered apoptotic. (J) Statistical analysis of the apoptosis rate across different groups. Error bars represent the mean±SEM. (K) The protein level of E-cadherin, Bax, Bcl-2 was measured in Eca109 and KYSE450 cells across different groups. The E-Cadherin, Bax, Actin was cropped from different parts of the same gel, and Bcl-2 was from different gels and from the same exposures. (L) Statistical analysis of the protein expression across different groups. Error bars represent the mean±SEM. Statistical analysis was generated from unpaired t-test, asterisks denote statistical significance as **p<0.001.

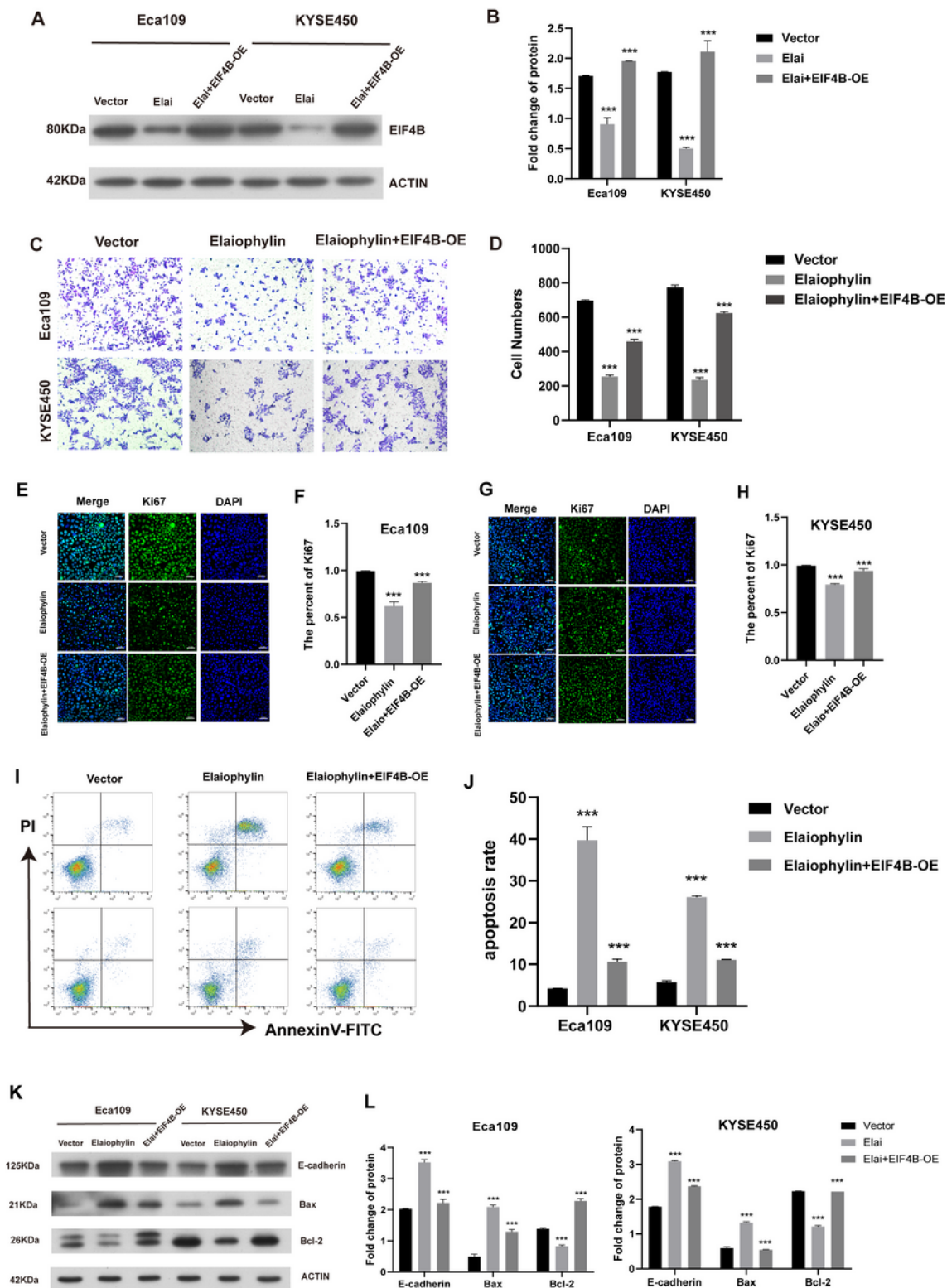


Figure 6

Upregulation of eIF4B could rescue the phenotype on ESCC cells caused by Elaiophylin. (A) Western blot examined the protein expression of EIF4B among different groups. (B) Statistical analysis of the protein expression of EIF4B. Error bars represent the mean±SEM. (C) Transwell assay measured the migration ability among different groups. (D) Statistical analysis of the cell numbers migrated to the other side of the chamber. Error bars represent the mean±SEM. (E, G) IHC of ki67 was used to detect the proliferation

rate of Eca109 and KYSE450 cells among different groups. (F, H). Statistical analysis result of the IHC showed that the ki67 expression level was downregulated in the Elaiophylin group compared with the control, and could be reversed by EIF4B-OE. Error bars represent the mean \pm SEM. (I) The apoptosis rate was measured by Annexin V/PI in Eca109 and KYSE450 cells. Cells with Annexin V-FITC positive and PI negative or both Annexin V-FITC and PI positive were considered apoptotic. (J) Statistical analysis of the apoptosis rate among different groups. Error bars represent the mean \pm SEM. (K) The protein level of E-cadherin, Bax, Bcl-2 was measured in Eca109 and KYSE450 cells among different groups. The E-Cadherin, Bax, Actin was cropped from different parts of the same gel, and Bcl-2 was from different gels and from the same exposures. (L) Statistical analysis of the protein expression among different groups. Error bars represent the mean \pm SEM. Statistical analysis was generated from unpaired t-test, asterisks denote statistical significance as **p \leq 0.001.

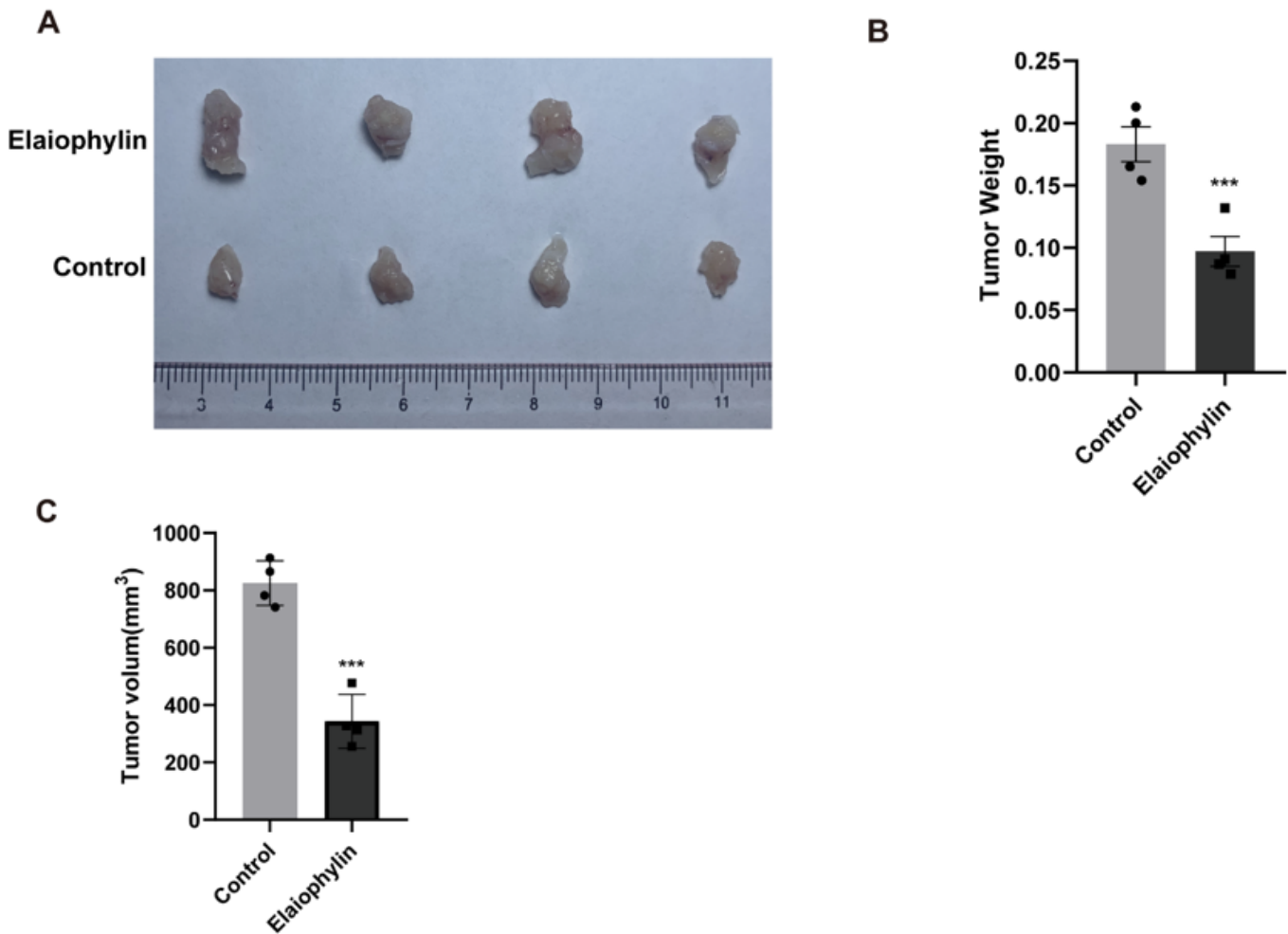


Figure 7

Elaiophylin inhibit the esophageal tumor growth in vivo. (A) The different groups of tumour were removed from the nude mice. (B) The weight of tumor of different groups. (c) The volume of tumor of different groups.

Supplementary Files

This is a list of supplementary files associated with this preprint. Click to download.

- [Figure1rawdata.tif](#)
- [figure2rawdata.tif](#)
- [Figure4rawdata.tif](#)
- [Figure5rawdata.tif](#)
- [figure6rawdata.tif](#)
- [Figure1rawdata.tif](#)
- [Figure4rawdata.tif](#)
- [Figure5rawdata.tif](#)
- [figure2rawdata.tif](#)
- [figure6rawdata.tif](#)